# Catalysis Science & Technology

Accepted Manuscript






ROYAL SOCIETY OF CHEMISTRY

www.rsc.org/catalysis

# Tunable acid-base bifunctional catalytic activity of FeOOH in an orthogonal tandem reaction

D. Vernekar and D. Jagadeesan*

Physical and Materials Chemistry Division

CSIR National Chemical Laboratory

Dr. Homi Bhabha Road

Pune – 411 008.

*Email: d.jagadeesan@ncl.res.in

Telephone: +91-020-2590 3046 Fax: +91-020-25902636.

**Abstract**

In this report, we have explored the acid-base bifunctional catalytic activity of Iron oxohydroxides (FeOOH) by catalyzing deacetalization and Henry condensation reactions successively in a single pot. The crystalline polymorphs of FeOOH namely goethite (α FeOOH), Akaganèite (β FeOOH), Lepidocrocite (γ FeOOH) and δ FeOOH were chemically prepared and tested for the catalytic activity. All the polymorphs of FeOOH exhibited acid-base bifunctional catalytic activity. The relative selectivity of products varied with the polymorphs of FeOOH. Whereas, α FeOOH produced benzaldehyde in high yield, the polymorphs β FeOOH, γ FeOOH and δ FeOOH showed a high selectivity for trans-β-nitrostyrene. In addition, β FeOOH also exhibited a unique activity towards the formation of 1,3-dinitro-2-phenylpropane. The difference in the catalytic activity of FeOOH polymorphs was explained based on the strength and density of acidic and basic active sites on the surface. Selectivity of the products was tuned by changing the synthesis parameters of the catalysts and reaction conditions.

Biosynthetic pathways in living organisms are excellent examples for tandem catalysis. A substrate is acted upon by enzymes in a sequential manner thereby efficiently pushing the chemical equilibrium towards products in high selectivity.[1,2] In the last decade, several attempts have been made to mimic nature's strategy on heterogeneous catalyst systems to develop multi-functional catalysts for orthogonal tandem reactions.[2,3] Multifunctional catalysts that are capable of carrying out orthogonal tandem reactions are important to the pharmaceutical industry in which significant savings on cost, energy and time can be achieved. From the materials perspective, a multifunctional catalyst must bear suitable active sites for each step of the tandem reaction. The active sites must be so positioned on the catalyst surface that they do not compromise their functions but act independently and sometimes co-operatively leading to a unique activity. Recently, nanostructured materials containing spatially isolated acidic and basic sites were found to be efficient as bifunctional catalysts for one-pot tandem reactions involving hydrolysis and condensation steps. The bifunctional nanomaterials were obtained by selectively functionalizing the outer and inner walls of hollow silica nanoparticles with acidic ($–SO_3H$ groups grafted on silica or -Si-OH groups) or basic (covalently anchored $-NH_2$) sites in a spatially separated manner.[4-6] Selectivity of products were tuned by controlling the chemical nature of acidic and basic sites and its location.[4-8] Distribution, stability and activity of the active sites were highly dependent on the method of synthesis such as co-condensation or post-synthesis grafting. However, major drawbacks of this method were the laborious steps of preparation and the use of toxic alkoxide reagents. Recently, acid-base bifunctional catalytic activity has been reported in organic-inorganic hybrid zeolites.[9,10] These catalysts exhibited acid property due to $Al^{3+}$ sites in zeolites and base sites due to the uncalcined organic structure directing agents. Besides the surface functionalized silica and hybrid zeolites, the literature of

bifunctional catalysts for tandem reactions is limited. This presents interesting challenges in materials chemistry to develop new materials with robust and efficient bifunctional active sites without spatially isolating acidic and basic groups on a surface. A number of acid – base equilibrium within a single species is well known in chemistry and a careful use of these systems can create bifunctional catalysts. The acidic and basic sites in such catalysts may be randomly distributed but will be useful as simple to produce without involving multiple steps of surface functionalization. It was our opinion that inorganic metastable phases such as metal oxohydroxides are ideal as robust, inexpensive and easily scalable acid-base bifunctional catalysts. These materials, which are usually prepared by hydrolytic sol-gel methods, can be considered as intermediates between hydroxylated metal sol precursors and completely condensed dense oxide phases. Iron oxohydroxides (FeOOH) are interesting candidates for bifunctional catalytic applications because of some of its unique features.[11] (i) Surface studies on FeOOH have shown FeOOH groups existing in chemical equilibrium with $FeOO^-$ as described in equation 1.

$$FeOOH + H_2O \leftrightarrow FeOO^- + H_3O^+ \text{----------} \rightarrow \text{(Eq. 1)}$$

It may be imagined that -OOH groups and its deprotonated conjugate base $–OO^-$ groups may be present in abundance on the surface and on the interiors of the material exhibiting acidic and basic properties respectively. (ii) FeOOH has been shown to possess three types of surface sites having different surface coordination. One may expect the p$K_a$ values of each of the species to be different. (iii) FeOOH is an abundantly available natural mineral and an important raw material in the pigment industry. Therefore, it is interesting to test the bifunctional catalytic activity of FeOOH in an industrially important tandem reaction. In this report, we have demonstrated the bifunctional property of FeOOH for the first time by catalyzing deacetalization and Henry

condensation reactions in tandem (Scheme 1). Interestingly, different crystalline polymorphs of FeOOH namely Goethite (α FeOOH), Akaganèite (β FeOOH), Lepidocrocite (γ FeOOH) and δ FeOOH showed different trends in the selectivity of products.

FeOOH catalysts were prepared using sol-gel reaction of iron salts and used without any further functionalization or activation (See ESI-1).[9,11-12] X-ray diffraction (XRD) patterns of the polymorphs of FeOOH in Fig. 1a were used to identify the crystalline structures. Each pattern could be indexed to a pure phase of FeOOH polymorph. δ FeOOH showed some traces of α $Fe_2O_3$. The FT-IR absorption spectra from traces (i) to (iv) in Fig. 1b also confirmed the composition of the polymorphs as α, β, γ and δ FeOOH respectively. FT-IR absorption bands due to Fe-O symmetric stretching and O-H bending vibrations occurring in the range of 620 - 680 $cm^{-1}$ and 750 - 1000 $cm^{-1}$ respectively were characteristic of FeOOH phases.[13-15] The synthesis conditions of the polymorphs did not employ any organic structure directing agent and therefore, the bulk particle morphology was consistent with the natural crystal growth under those pH conditions. Morphology and microstructure of FeOOH polymorphs were studied using scanning electron microscopy (SEM) and transmission electron microscopy (TEM) respectively. The SEM and TEM images of α FeOOH (Fig. 2a &b) showed rod shaped microstructures which were 100 – 300 nm in diameter and 250 nm - 1μm in length. In Fig. 2d & 2e, β FeOOH showed more uniform rod shaped structures with smaller aspect ratio. The diameter was in the range of 60 nm and length was around 350 nm. Elemental analysis of β FeOOH showed the presence of $Cl^-$ ions that are essential for stabilizing the crystal structure. γ FeOOH had a layered morphology which was recognized from the shape of the crystals observed using SEM (Fig. 2g). In Fig. 2h the layers that are standing on its edge can be observed. SEM and TEM images in Fig. 2j & Fig. 2k showed nanoparticles of δ FeOOH which were in the range of 10 – 20 nm. In Figs. 2c, 2f and 2i,

the crystal structure models of α, β and γ FeOOH showing the arrangement of $Fe(O,OH)_6$ octahedra are shown. In δ FeOOH, anions and cations are distributed almost randomly and without a definite arrangement of the octahedra. Textural properties of the FeOOH polymorphs were probed using $N_2$ adsorption isotherms and the results are shown in Fig. 3 and Table 1. BET surface area of the polymorphs differed widely depending on the microstructure of the material. γ FeOOH which had a layered structure exhibited the highest surface area of 247 $m^2g^{-1}$ and α FeOOH with micron sized rod like structures exhibited 24 $m^2g^{-1}$. The hysteresis observed could be due to inter particle spaces.

FeOOH polymorphs were tested for their catalytic activity in deacetalization – Henry reaction as shown in the scheme 1 (see ESI 1). Mechanistically, benzaldehyde dimethylacetal (**1**) was hydrolysed to form benzaldehyde (**2**) in the presence of an acid catalyst, which further underwent a base-catalyzed Henry condensation with $CH_3NO_2$ to form 2-nitro-1-phenylethanol (**3**). Dehydration of **3** forms trans-β-nitrostyrene (**4**). In the presence of a base, **3** could further undergo a Michael addition reaction with another molecule of $CH_3NO_2$ to form 1,3-dinitro-2-phenylpropane (**5**). In Fig. 4a, the conversion of **1** catalyzed by various polymorphs of FeOOH is shown. In the absence of catalyst, the reaction proceeded at 5% conversion with **2** as the only product. On the other hand, α FeOOH showed a conversion of 52%, and the average conversions of β, γ, and δ FeOOH were over 94 %. The difference in the levels of conversion by the polymorphs of FeOOH could be correlated with the surface area and the morphology of the catalysts. For example, α FeOOH with a low surface area showed only modest levels of conversion in comparison with other polymorphs. The morphology of the catalysts could have had an important role in the catalytic activity of the polymorphs. The occurrence of α FeOOH as micrometer sized particles with a much lower surface to volume ratio compared to other

polymorphs is clearly reflected in its performance. In addition, the denser octahedral packing of α FeOOH could have limited the accessibility of the active sites for the reactant molecules. On the other hand, nanostructured morphology of other polymorphs must have had an advantage in terms of higher surface to volume ratio and accessibility to active sites. Besides, nanorods of β FeOOH crystals are also less dense than α and γ FeOOH due to its body centered packing of anions with intra crystalline tunnels. γ FeOOH with layered morphology exhibited an interlayer spacing of 2 - 3 nm and a very high surface area. Diffusion of molecules to the active sites along the (100) planes could be easily facilitated through interlayer spacing. In Fig. 4b, formation of products **2**, **3, 4** and **5** catalyzed by polymorphs of FeOOH are shown. It was interesting to note the formation of **4** and **5** (Fig. 4b). Earlier works have shown that mono-functional acidic or basic catalyst cannot form the **3**, **4** or **5** starting from **1**.[16] Formation of **4** and **5** strongly suggested the presence of acidic and basic sites on the catalyst surface. An interesting observation was that the relative ratio of the products formed by each polymorph was different as shown in Fig. 4b. For instance, α FeOOH showed a higher selectivity for **2**, while all other polymorphs formed **4** as the major product. Product **3** could not be observed under the reaction conditions. Interestingly, β FeOOH displayed a unique activity by forming **5** in relatively larger amount than other polymorphs. The products **4** and **5** are important in the synthesis of pharmaceutical products, fungicides, and herbicides.[17-20] Therefore, a catalyst with a high selectivity to any of these products is highly desirable. Among the polymorphs, γ and δ FeOOH formed **4** as the major product. In a similar way, the catalytic activities of FeOOH polymorphs were studied for Henry reaction starting from **4** as the reactant. The motivation was to study the catalytic behavior of the polymorphs for base-only catalyzed Henry reaction. In ESI 2, the conversion of **2** is shown for

various polymorphs. The conversion and yield of products such as **3**, **4** and **5** were similar in trend to the deacetalization-Henry reaction.

In Table 2, the results of the reaction catalyzed by γ and δ FeOOH are presented. Entries 1 to 4 represent the results of the reactions that were carried out for different duration of time. The yield of **4** was around 93% at the end of 48 h using γ and δ FeOOH. The difference in the active sites on the surface of FeOOH polymorphs became prominent when the reaction was carried out under different conditions. Thus, on decreasing the reaction duration to 12 h, γ FeOOH showed a further improvement in the yield of **4** to 97.5%, while δ FeOOH did not show any improvement. It is interesting to note that although the activity of γ and δ FeOOH was similar at 48 h, there was a significant difference in the activity when the reaction was carried out for 12 h. From XRD data in Fig. 1a, δ FeOOH showed some traces of α $Fe_2O_3$. However, the observed catalytic behavior of δ FeOOH did not have any influence of α $Fe_2O_3$ as the impurity phase mainly gave only **2** in the control experiments under the same conditions. Both γ and δ FeOOH did not form **3** under the reaction conditions. Even under milder conditions at 80 $^oC$, **3** was not observed probably because the acidic sites on FeOOH were active in dehydration of **3** to **4**. Our attempts to tune the yield of **5** using β FeOOH are shown in Table 3. We assumed that a relatively higher selectivity for **5** could be related to the presence of $Cl^-$ ion in the structure. Accordingly, we prepared β FeOOH with different concentrations of $Cl^-$ ions without affecting the crystal structure and carried out the reaction under same conditions. As shown in entries 1 to 3 in Table 3, a volcanic relation was observed between the $Cl^-$ ion concentration and the yield of **5** (relative to **4**). Structural analysis of the used β FeOOH catalysts by XRD did not show any significant leaching of $Cl^-$ ions. Expecting a dramatic enhancement in the yield of **5**, we

exchanged 50% of $Cl^-$ ions with more basic $OH^-$ ions. However, the result did not show any marked difference.

In order to show the acid-base catalyzed reaction pathway of the catalysts, we chose β and γ FeOOH catalyzed reactions and analyzed the products at different time intervals. The reason for choosing these two catalysts was their unique and diverse activity. In Figs. 5a & 5b, the yield (%) of **1**, **2**, **4** and **5** found in the reaction medium catalyzed by β and γ FeOOH are plotted against time. It was clearly observed that the yield of starting material **1** decreased with time, while that of **2** increased with time initially but decreased eventually. The decrease in the yield of **2** was accompanied by the increase of **4** in case of γ FeOOH. Similarly in case of β FeOOH, an increase in the yield of **4** and **5** occurred with the gradual decrease in the yield of **2**. The observation suggested that **1** was hydrolyzed to **2** progressively with time which underwent condensation with $CH_3NO_2$ to form products **4** and **5**. In the presence of externally added pyridine molecule, a decrease in the conversion to 63% was observed in deacetalization-Henry reaction confirming the role of acidic sites in initiating the first step of the reaction. Thus, acid-base catalyzed reaction pathway starting from **1** going to **3**, **4** and **5** via **2** as an intermediate is proved beyond doubt. It is likely that during the reaction, Fe metal ions leached out of the solid FeOOH and behaved as a catalyst for the conversion of **1** to other products such as **2**, **3**, **4** or **5**. In order to prove the heterogeneous nature of FeOOH catalysis in deactalization-Henry reaction, we carried out the reaction using β and γ FeOOH starting from **1**. The reaction was carried out for 4 h in the presence of the catalyst during which a conversion of 40 - 50% was observed with respect to **1**. At this stage, only product **2** was observed in case of both β and γ FeOOH. Following this, the catalysts were quickly removed by centrifuge and the remaining reaction liquid containing 1, 2, $CH_3NO_2$ and a small amount of $H_2O$ was subjected to reflux for another

44 h under $N_2$ atmosphere. The results at the end of 44 h are presented in ESI 3. It can be observed that in the absence of solid FeOOH (β and γ) catalysts, the conversion of the reaction increased only slightly with respect to **1**. However, the base catalyzed step of the tandem reaction did not proceed at a faster rate. ICP analysis of the reaction medium at the end of the reaction revealed the presence of 0.39 and 6.7 $mgL^{-1}$ of Fe metal. A meager 2 - 8 % increase in the yield of **4** after the duration of 44 h could be due to activity of small colloidal nanoparticles of FeOOH that did not settle down by centrifuge. The experiment clearly proved that the catalytic sites were indeed present on the solid surface of FeOOH catalysts.

The presence of acid-base bifunctional sites on FeOOH and its application as catalyst for tandem reaction is an important aspect in this work as it is reported for the first time. The chemical equilibrium existing on the surface of FeOOH according to the Eq.1 is probably responsible for the presence of acidic and basic sites. The surface -OOH groups on FeOOH acts as a Brønsted acid and its conjugate base $FeO^-$ behaves as a Brønsted base. In order to establish the role of $H_2O$, we carried out control experiments using γ FeOOH as the catalyst. In the absence of $H_2O$, the conversion was found to decrease drastically to 52% (95% in the presence of $H_2O$). This observation proved that the rate of reaction decreased in the absence of $H_2O$. On analyzing, it was observed that the yield of **2** was dominant in the absence of $H_2O$ as compared to in the presence of $H_2O$. A similar kind of behavior was observed in Henry reaction starting from benzaldehyde using γ FeOOH as the catalyst. In the presence of water, we observed 94% conversion while only 49% conversion was observed in the absence of $H_2O$. The significant amount of conversion even in the absence of external $H_2O$ was surprising. Thermogravimetric analysis (Fig. 6) of the polymorphs however revealed that surface adsorbed moisture accounted for nearly 10 – 20 % weight loss in the temperature range below 200 $^oC$ which could have played

the necessary role in the hydrolysis step of the reaction. Thus, $H_2O$ is crucial role in the creation of both acidic and basic sites on the catalyst which were responsible for catalyzing the tandem reaction. In Scheme 3, the mechanism of reaction on the surface of FeOOH is summarized. Step 1 involves the acid (FeOOH) catalyzed deacetalization reaction forming **2** while step step 2 shows the base (FeOO-) catalyzed condensation reaction leading to the formation of products **3**, **4** and **5**.

In order to probe the nature of the acid and base sites, pyridine was adsorbed on FeOOH samples and FT-IR spectra were recorded (Fig. 7). The absorption bands of the FT-IR spectra in the range 1515-1565 $cm^{-1}$ was attributed to the Brønsted acid protons while Lewis acidic sites were detected in the range 1435-1470 $cm^{-1}$. All polymorphs showed at least three prominent bands in this region around 1560, 1541 and 1508 $cm^{-1}$ which was attributed to the formation of pyridinium ion due to Brønsted acid sites. The band at 1457 $cm^{-1}$ could be attributed to the adduct formed by pyridine with the Lewis acidic $Fe^{3+}$.[21,22] Strength of acidic and basic sites and their density on the surface was estimated by acid-base titrations using Hammett indicators of different $H_0$ values. (See ESI 1) The acidity value is represented as the number of acid sites ($mmolg^{-1}$) whose acid strength is equal to or less than the $H_0$ value (of the indicator) and the basicity as the number of basic sites ($mmolg^{-1}$) whose base strength is equal to or greater than the $H_0$ value (of the indicator). Acidity and basicity are tabulated on a common $H_0$ scale using an already reported procedure.[23] Low $H_0$ value referred to a strongly acidic site and a high $H_0$ value represented a strongly basic site. In Table 4, we show the surface acidity and basicity values on a common $H_0$ value for all the FeOOH polymorphs. The polymorphs showed a high number of acid sites of various strengths. The numbers of acid sites were comparatively higher than the number of basic sites which could probably mean a low equilibrium constant of reaction in eq.

The presence of acid and base sites of different strengths may be due to different types of –OOH groups on the surface of the catalysts. The strengths of –OOH groups could vary due to differences in coordination numbers of O atoms and intermolecular H-bonding specific to the crystal structure. Theoretical calculations have identified at least three sites with different coordination of oxygen atom (Scheme 2).[24-26] The results presented in Table 4 are useful to understand the difference in the selectivity of products obtained using FeOOH catalysts. For example, α FeOOH possessed maximum number of acid sites and least number of basic sites among the polymorphs of FeOOH. Thus, α FeOOH always formed only **2** as the major product as the basic sites were not enough in strength and number to catalyze Henry reaction. Although α FeOOH had strong acid sites, the dense crystal structure with a low surface area resulted in poor conversion. Other FeOOH polymorphs possessed both acidic and basic sites and therefore could form condensation products **4** and **5**. Similar trends in the conversion and yield of products were observed for FeOOH polymorphs in Henry reaction (ESI 2). Interestingly, α FeOOH which formed only 2 in deacetalization –Henry reaction showed the selectivity for 4 in Henry reaction although only less than 20%. This is in agreement with our assumption α FeOOH is predominantly acidic but has some basic sites at $H_0$ = 1.5 present. However, considering the number of active sites (acid and base), TOF for Henry reaction was higher by two orders of magnitude compared to TOF of deacetalization-Henry reaction. TOF ($h^{-1}$) of the catalysts for deacetalization Henry reaction are as follows α FeOOH ($3.8\times10^{-2}$), β FeOOH ($6.9\times10^{-2}$), γ FeOOH ($7.3\times10^{-2}$) and δ FeOOH ($7.9\times10^{-2}$). TOF ($h^{-1}$) for Henry reaction are as follows α FeOOH (2.5), β FeOOH (1.5), γ FeOOH (4.2) and δ FeOOH (1.5).

Another interesting observation in Table 2 was that γ and δ FeOOH, which showed a similar activity (conversion and selectivity) at 48 h differed much at the end of 12 h. This

observation suggests that γ FeOOH possessed more number of accessible active sites than δ FeOOH which is clearly evident from the values of acidity and basicity shown in Table 4. The formation of **5** in case of β FeOOH was interesting. The formation of product **5** needs stronger basic sites because of the Michael addition of product **4** with $CH_3NO_2$. The presence of trace amounts of strong basic sites of $H_0 = 6.8$ in β FeOOH is probably responsible for the enhanced selectivity of **5** by β FeOOH. The unique feature of β FeOOH is the presence of $Cl^-$ ions. The -OH groups are directed towards the centre of the tunnel which is stabilized by $Cl^-$ ions. Attempts to improve the selectivity by replacing the $Cl^-$ ion with more basic $OH^-$ ions did not have much effect. This suggested that the location of $Cl^-$ or $OH^-$ ions were most likely inaccessible to the reactants. However, it is possible that the strong basic sites on β FeOOH could be because of the H-bonding interactions involving $Cl^-$ ions in the crystal structure. Further studies are needed to understand this aspect clearly.

The stability of the catalysts was studied for β and γ FeOOH and the data is shown in Fig. 8. The recyclability data of β and γ FeOOH with conversion (with respect to 1 in 12 h) along with the selectivity of product 4 is plotted as Fig. 8a and b respectively. β FeOOH showed a significant decrease in the conversion from second cycle onwards (black bars in Fig. 8a) and seemed to recover. However, elemental analysis showed only 0.39 $mgL^{-1}$ of Fe in the reaction medium which is insignificant. XRD and TEM analysis confirmed the stability of the crystal structure of β FeOOH even after five cycles (See ESI 4 and ESI 5) suggesting no significant loss of $Cl^-$ ion. On estimating the acid and base functional groups by titrations, it was observed that there was a considerable decrease in the values of surface acidic groups. Certainly, the drastic loss in the levels of conversion could be related to the low values of active sites. FT- IR absorption data used β FeOOH (after one cycle) was recorded and compared with that of the

fresh catalyst (ESI 6). We could observe the appearance of new absorption bands in the region 1400 $cm^{-1}$ suggesting the presence of aromatic C=C functional groups on the used β FeOOH catalysts. Among the polymorphs, β FeOOH possessed intra crystalline channels of diameter close to 0.8 nm which may be suitable for the diffusion of small molecules such as $CH_3NO_2$. However, after reaction, the diffusion of condensation products such as **3**, **4** or **5** away from the active sites could be slower. It is possible that the larger molecules could strongly interact with the acid sites causing deactivation. In order to confirm this, we carried out TGA of used β FeOOH and compared it to the fresh sample. Although we did not find any significant weight loss due to adsorbed organic molecules as we suspected, we observed a reduced weight loss in the temperature region 250 – 400 $^oC$ which is due to loss of $Cl^-$ ions. TGA data suggested that used β FeOOH had lesser amount of $Cl^-$ ion compared to the fresh sample but not low enough to affect the structural stability. However, it appears that the loss in $Cl^-$ ion has had its impact in the strength of the acid-base sites and hence the levels of conversion. It must also be noted that although the level of conversion (with respect to 1) seemed to recover by 5-15 % after 2$^{nd}$ cycle, the loss in the selectivity of **4** does not follow the suit. The exact reason for the recovery in conversion of 1 in β FeOOH is not clear. On the other hand, γ FeOOH showed a relatively stable level of conversion with respect to 1 even after five cycles of reaction (Fig. 8b). The selectivity of **4** was maintained more or less at the same level. XRD pattern and TEM image of the sample after five cycles of reactions showed no changes in the crystalline structure (See ESI 4 and ESI 5).

In conclusion, the acid-base bi-functional catalytic activity of the polymorphs of FeOOH namely α, β, γ and δ is described for the first time. The polymorphs exhibited different selectivity of products which could be tuned to some extent by changing the time of reaction and sample

composition. The origin of acid and base bifunctional property is due to the surface chemical equilibrium between FeOOH and $FeOO^-$ groups. The difference in the selectivity with the polymorphs is probably due to the different types of FeOOH sites and the density of the sites present on the crystal facets of the polymorphs. The work assumes significance because it describes the bifunctional aspects of FeOOH polymorphs and demonstrates the practical applications for deacetalization-Henry reaction. The catalytic property of FeOOH also suggests the potential bifunctionality of other hydroxylated metal oxides. It is hoped that the new property of this naturally available mineral will open doors for further applications.

**Acknowledgement**

DJ acknowledges the financial support of Ramanujan Fellowship (RJN-112/2012) by SERB. DV acknowledges DST - INSPIRE doctoral Fellowship. The authors thank Mr. S. Gupta, Dr. C. S. Gopinath, Dr. K. Sreekumar and Centre for Materials Characterization in CSIR-NCL for sample characterization. The authors also thank Dr. A. Nag and Dr. R. Vaidyanathan from IISER-Pune for characterizing the samples. Elemental analysis was performed at the DBT-BIRAC supported Venture Centre at CSIR-NCL, Pune, India.

**Notes and references**

1. I. Oroz-Guinea and E. García-Junceda, *Curr. Opin. Chem. Biol*., 2013, **17**, 236-249.
2. J. M. Lee, Y. Na, H. Han and S. Chang, *Chem. Soc.Rev.*, 2004, **33**, 302–312.
3. M. J. Climent, A. Corma, S. Iborra and M. J. Sabater, *Green Chemistry*, 2014, **4**, 870-891.
4. S. Huh, H-T. Chen, J. W. Wiench, M. Pruski and V. S.-Y. Lin, *Angew. Chem., Int. Ed.*, 2005, **44**, 1826 –1830.
5. U. Diaz, D. Brunel and A. Corma, *Chem. Soc. Rev.*, 2013, **42**, 4083-4097.
6. K. Motokura, M. Tomita, M. Tada and Y. Iwasawa, *Chem. Eur. J*., 2008, **14**, 4017-4027.

7. B. Liu, H. Liu, C. Wang, L Liu, S. Wu, J. Guan and Q. Kan, *Appl. Catal. A*, 2012, **443–444**, 1-7.
8. E. L. Margelefsky, R. K. Zeidan and M. E. Davis, *Chem. Soc. Rev*., 2008, **37**, 1118–1126.
9. L. Xu, C Li, K Zhang and P Wu, *ACS Catal.* 2014, **4**, 2959 −2968.
10. A. Corma, U. Dȋaz, T. Garcȋa, G.Sastre, and A. Velty, *J. Amer. Chem. Soc.,* 2010*,* **132**, 15011-15021.
11. R. M. Cornell and U. Schwertmann, in *The Iron Oxides*, Wiley-VCH Verlag GmbH & Co. KGaA, 2003, pp. 222-228.
12. G. Lee, S. Kim, B. Choi, S. Huh, Y. Chang, B. Kim, J. Park and S. J. Oh, *J. Korean Phys. Soc*., 2004**, 45**, 1019 –1024.
13. P. Cambier, *Clay Min.,* 1986, **21**, 191-200.
14. E. Murad and J. Bishop, *Am. Min*., 2000, **85**, 716-721.
15. S. Okamoto, *Am. Ceram. Soc.,* 1968, **51**, 594-599.
16. P. Li, C. Cao, Z. Chen, H. Liu, Y. Yu and W. Song, *Chem. Commun.,* 2012, **48**, 10541–10543.
17. D. Y. Park, K. Y. Lee and J. N. Kim, *Tetrahedron Lett*., 2007, **48**, 1633-1636.
18. S B. Tsogoeva, *Eur. J. Org. Chem*., 2007, **11**, 1701–1716.
19. N. Milhazes, R. Calheiros, M. Marques, J. Garrido, M. Cordeiro, C. Rodrigues, S. Quinteira, C. Novais, L. Peixe and F. Borges, *Bioorg. Med. Chem*., 2006, **14**, 4078 –4088.
20. J. M. Betancort, and C. F. Barbas, *Org. Lett.* 2001, **3**, 3737–3740.
21. D. Yazici and C. Bilgic, *Surf. Inter. Anal.,* 2010, **42**, 959 - 962.
22. M. Yurdakoc, M. Akcay, Y. Tonbul and K. Yurdakoc, *Turk. J .Chem.,* 1999, **23**, 319 - 327.
23. T. Yamanaka and K. Tanabe, *J. Phys. Chem.*, 1976, **80**, 1723 −1727.

24. P. Venema, T. Hiemstra, P. Weidler, and W. Riemsdijk, *J. Colloid Interface Sci.*, 1998, **198**, 282-295.

25. T. Hiemstra, P. Venema and W. Riemsdijk, *J. Colloid Interface Sci.,* 1996, **184**, 680 – 692.

26. V. Barron and J. Torrent, *J. Colloid Interface Sci.,* 1996, **117**, 407 - 411.

## Schemes

**Scheme1**: Deacetalization – Henry condensation reaction: Structures of products benzaldehyde dimethylacetal (**1**), benzaldehyde (**2**), 2-nitro-1-phenylethanol (**3**), trans-β-Nitrostyrene (**4**) and 1,3-dinitro-2-phenylpropane (**5**) are schematically shown.

**Scheme 2**: Representation of different types of surface hydroxyl groups on FeOOH in a) single b) double and c) triple coordinated modes

**Scheme 3**: Mechanism of deacetalization-Henry condensation reaction occurring on the surface of FeOOH.

## List of Figures

**Fig. 1**: **a**) XRD patterns of FeOOH, **b**) FT-IR spectra of FeOOH polymorphs. Traces (i) α FeOOH, (ii) β FeOOH, (iii) γ FeOOH and (iv) δ FeOOH. * Peaks due to α $Fe_2O_3$.

**Fig 2**: SEM images (**a, d, g** and **j**) and TEM images (**b, e, h** and **k**) and crystal structures (**c, f** and **i**) of the FeOOH polymorphs are shown. (**a, b, c**) α FeOOH, (**d, e, f**) β FeOOH, (**g, h, i**) γ FeOOH, and (**j, k**) δ FeOOH. The crystal structures were taken from the website http://shalaleh.blogfa.com/.

**Fig. 3**: Nitrogen adsorption-desorption isotherms of FeOOH polymorphs. Traces (i) (●) α FeOOH, (ii) (○) β FeOOH , (iii) (■) δ FeOOH and (iv) (□) γ FeOOH

**Fig. 4**: a) Conversion of deacetalization – Henry condensation reaction of different polymorphs of FeOOH, b) Selectivity yield of products (**2**, **3**, **4** and **5**) obtained from catalysts α FeOOH, β FeOOH, γ FeOOH and δ FeOOH. Reaction was carried out under reflux conditions in $CH_3NO_2$ for 48 h.

**Fig. 5**: Time dependent product distribution of (a) β FeOOH and (b) γ FeOOH catalysts. (■) Reactant 1, (●) Product **2**, (□) Product **4** and (○) Product **5**.

**Fig. 6**: Thermogravimetric analysis data for the polymorphs Traces (i) β FeOOH, (ii) γ FeOOH, (iii) δ FeOOH and (iv) α FeOOH.

**Fig. 7**: FT-IR spectra polymorphs of FeOOH adsorbed with pyridine. Traces (i) α FeOOH, (ii) β FeOOH, (iii) γ FeOOH, (iv) δ FeOOH

**Fig. 8**: Reusability studies of (a) β FeOOH, where Conversion % with respect to 1(■) and selectivity for 4 (■) and (b) γ FeOOH, where conversion with respect to 1 (■) and selectivity with respect to 4 (■) for deacetalization-Henry reaction at 105 $^{o}$C for 12 h are plotted.

**List of Tables**

**Table 1**: Textural parameters of FeOOH polymorphs as determined by BET equation.

**Table 2:** Table showing the conversion and selectivity of γ and δ FeOOH catalysts.

**Table 3:** Table showing the conversion and selectivity of β FeOOH catalyst.

**Table 4**: Strength and density of acid and base sites on FeOOH catalysts determined using Hammett indicators.

**Scheme 1**

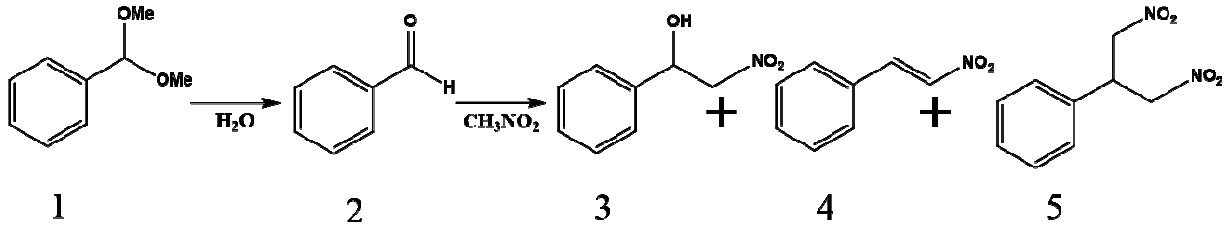


1 2 3 4 5

**Scheme 2**

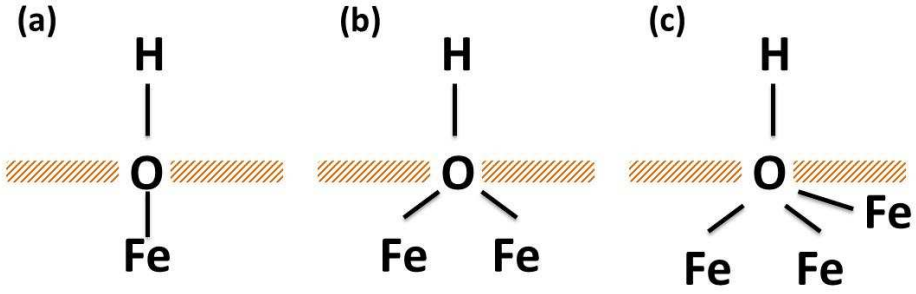

Scheme 3

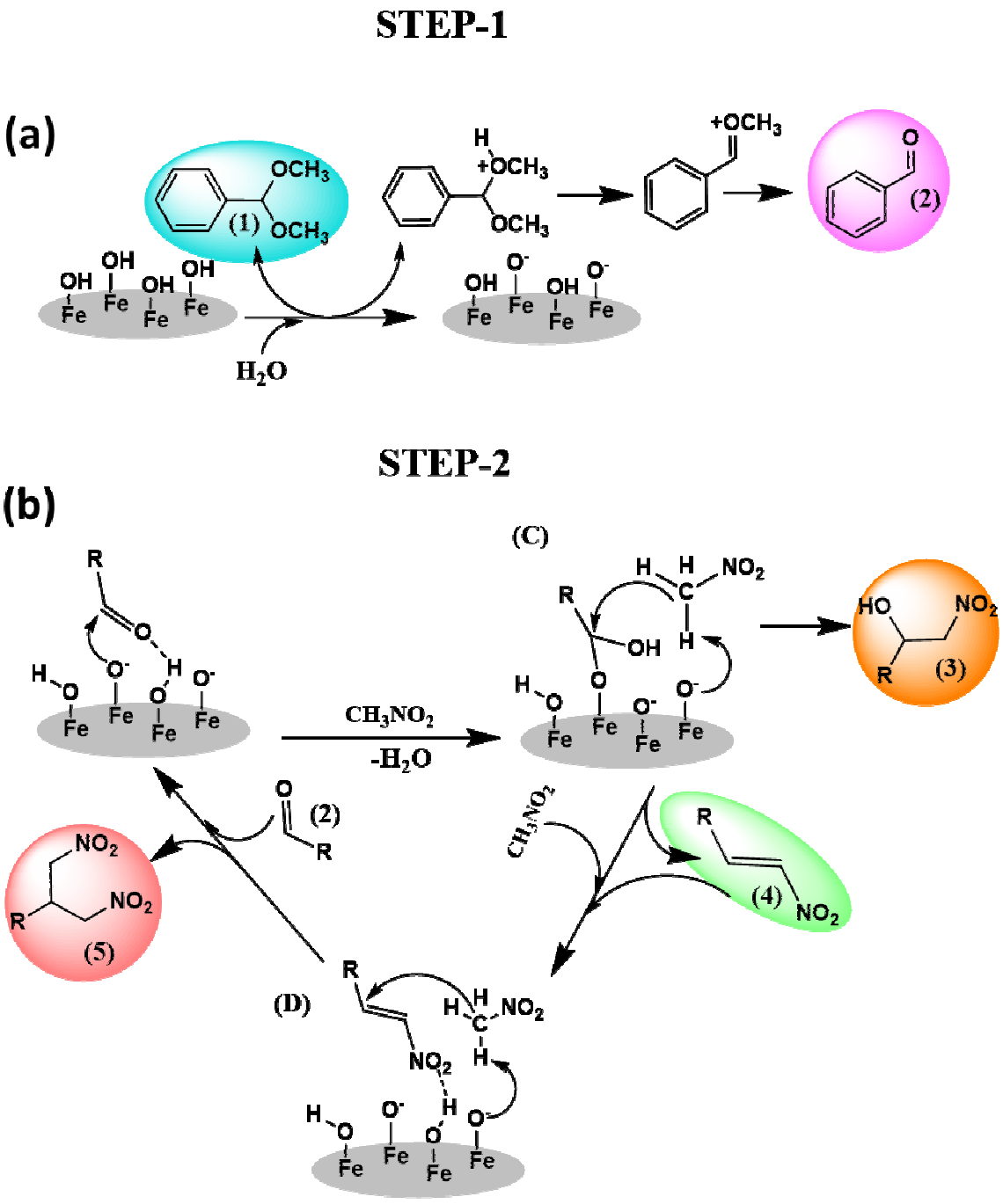

Fig. 1

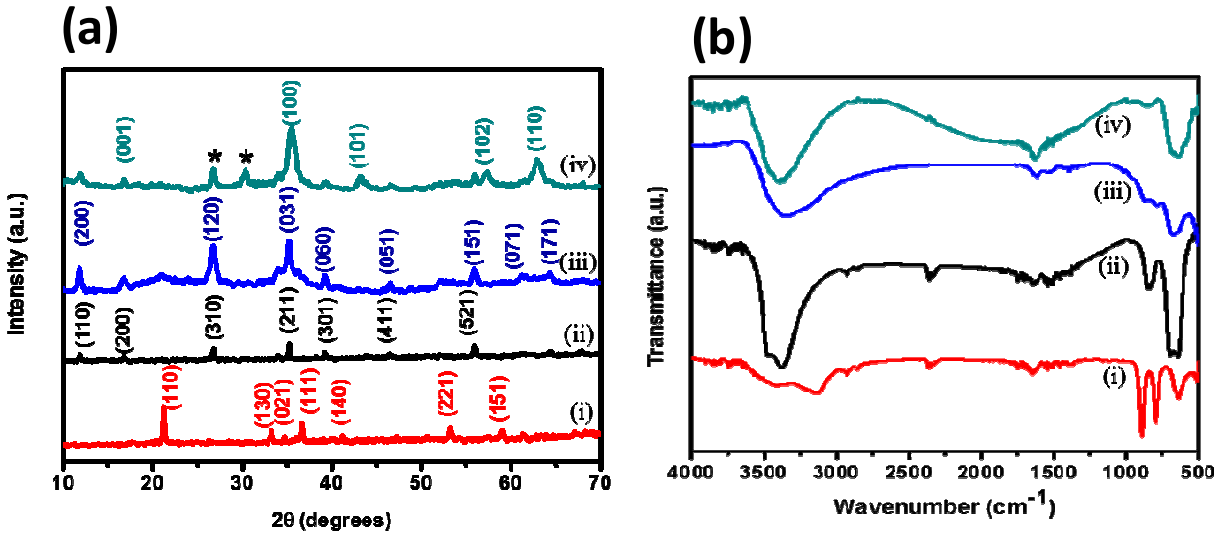

**Fig. 2**

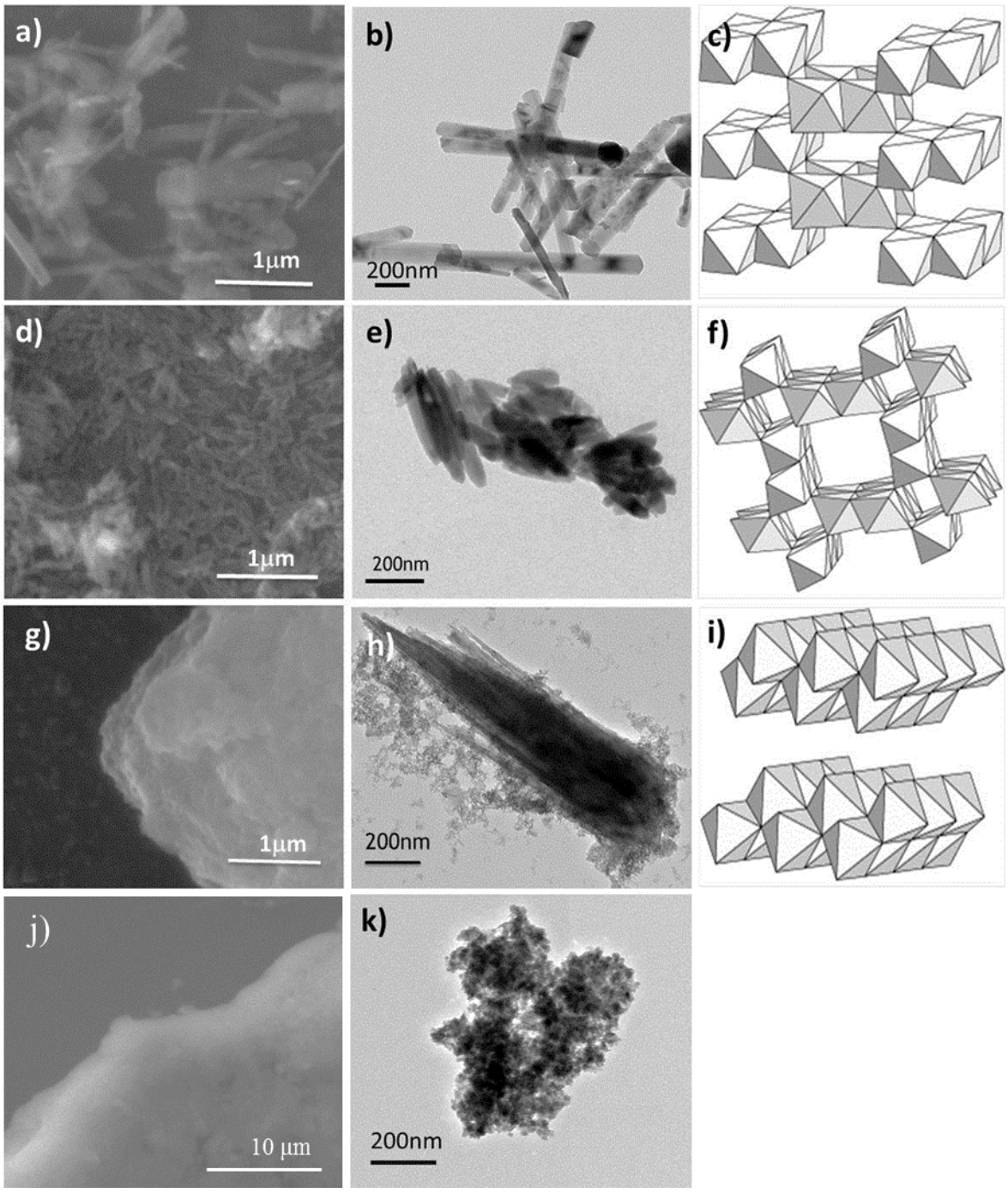

Fig. 3

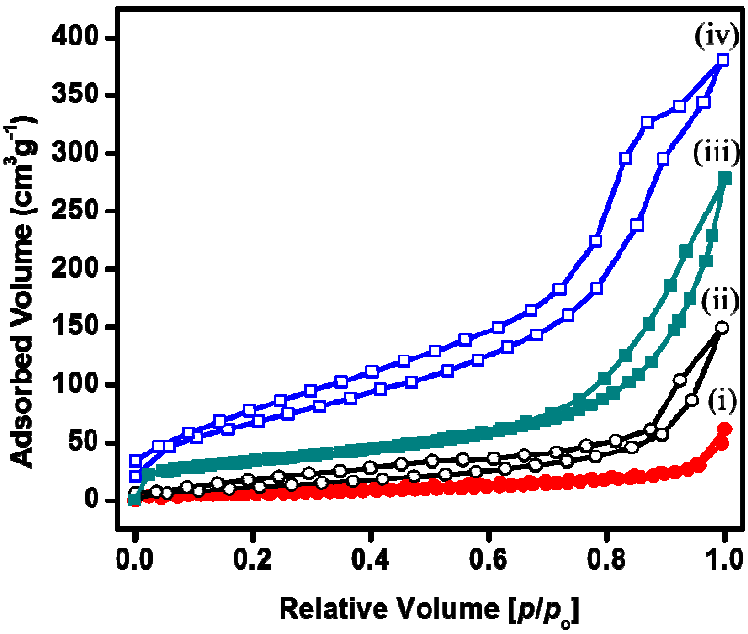

**Fig. 4**

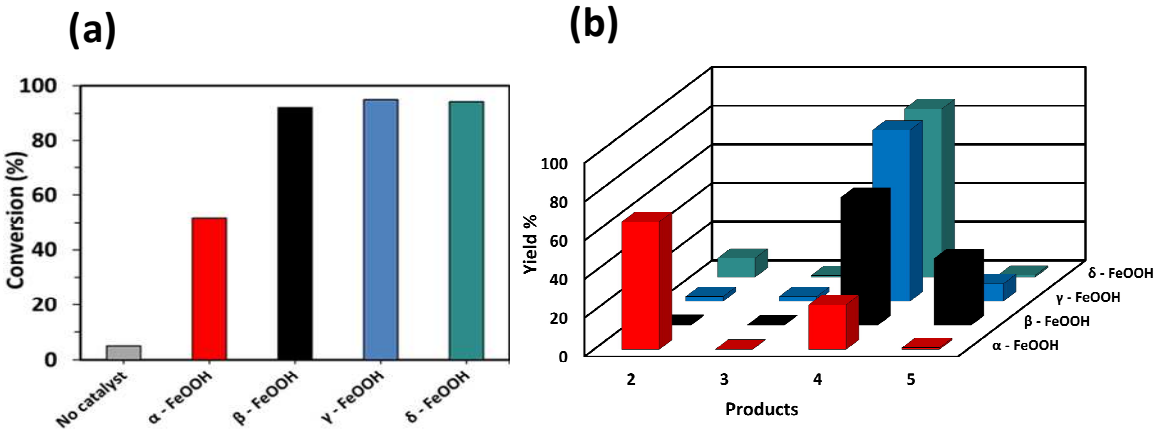

Fig. 5

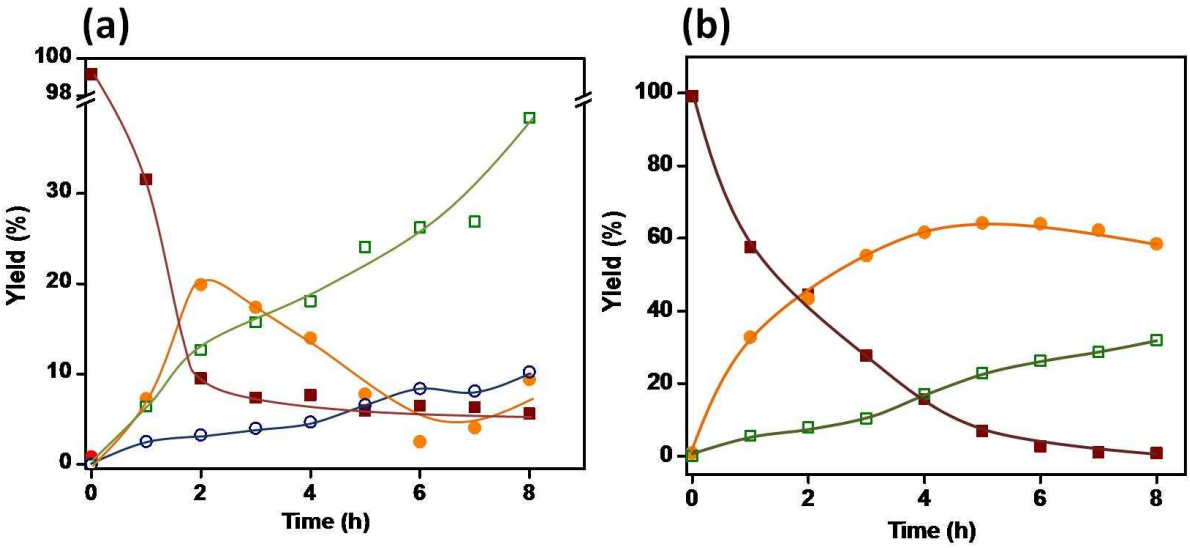

**Fig. 6**

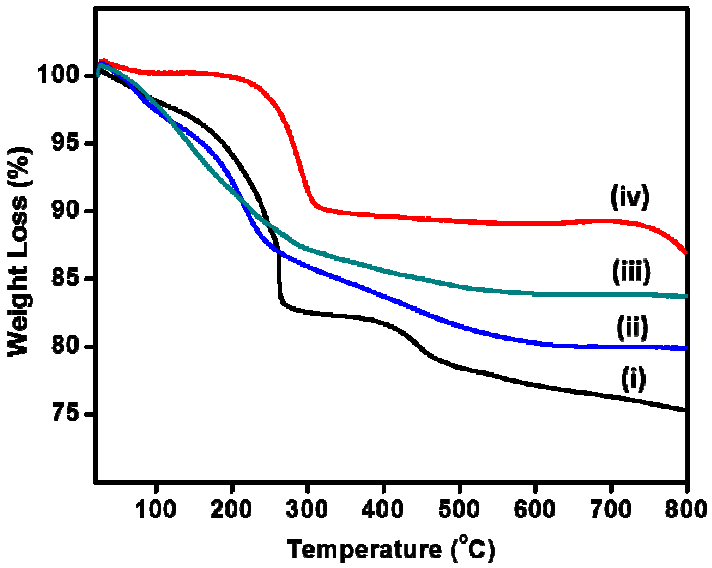

Fig. 7

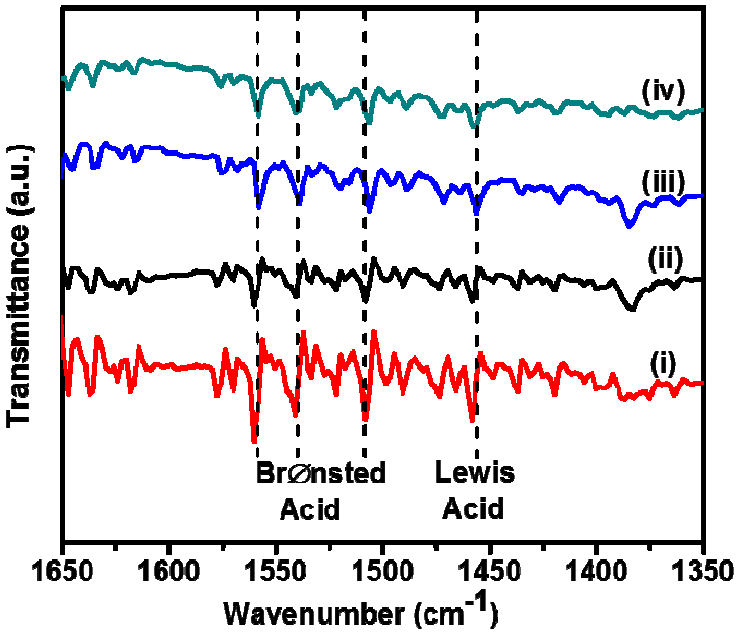

**Fig. 8**

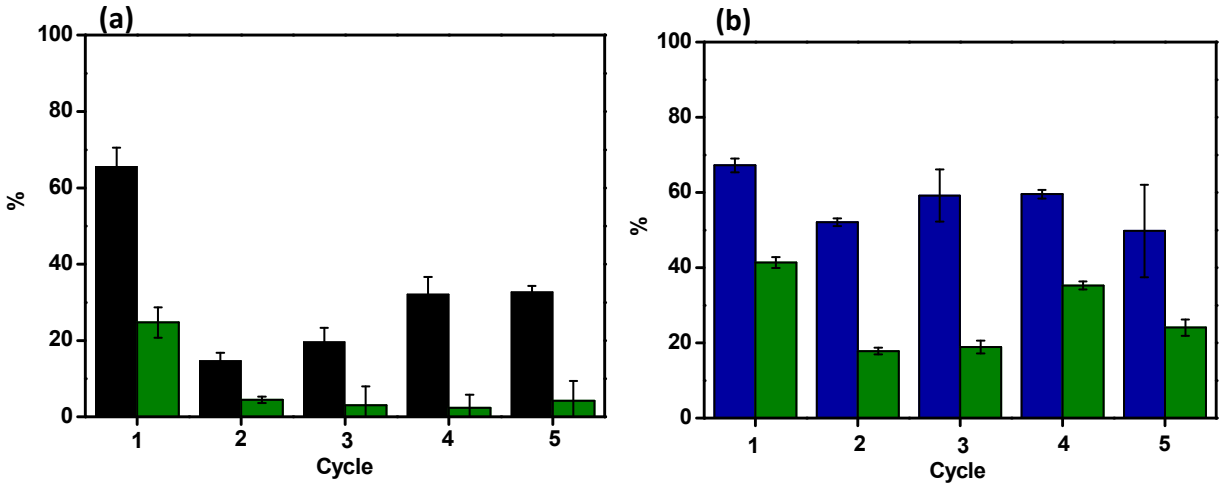

**Table 1**

| S. No | Polymorph | Surface area $m^2g^{-1}$ | Pore volume $ccg^{-1}$ | Pore radius Å |
|---|---|---|---|---|
| 1 | α FeOOH | 24 | 0.05 | 13.8 |
| 2 | β FeOOH | 44 | 0.23 | 17.9 |
| 3 | γ FeOOH | 247 | 0.58 | 15.8 |
| 4 | δ FeOOH | 123 | 0.32 | 7.0 |

**Table 2**

| S.No | Catalyst | Time (h) | Temperature ($^{o}$C) | Conversion (%) | Yield (%) | |
|---|---|---|---|---|---|---|
| | | | | | Product 2 | Product 4 |
| 1 | γ FeOOH | 48 | 105 | 95 | 2.5 | 93 |
| 2 | γ FeOOH | 12 | 105 | 86 | 0.6 | 97.5 |
| 3 | δ FeOOH | 48 | 105 | 94 | 6 | 93 |
| 4 | δ FeOOH | 12 | 105 | 88 | 21.7 | 77.7 |
| 5 | γ FeOOH | 12 | 80 | 71 | 57 | 41.6 |

Reaction conditions: Weight of the catalyst is 0.1 g, 3 mmol of benzaldehyde dimethylacetal, 2 mL of $CH_3NO_2$ and 3mmol of $H_2O$. Trace amounts of 5 is also observed. All reactions were carried out in $N_2$ atmosphere.

**Table 3**

| S.No | Catalyst | [$Cl^-$] (At %) | Conversion (%) | Yield ratio Product5 : Product4 |
|---|---|---|---|---|
| 1 | β FeOOH | 1 | 84 | 0.1 |
| 2 | β FeOOH | 4 | 95 | 1.9 |
| 3 | β FeOOH | 6 | 92 | 0.5 |
| 4 | β FeOOH ($OH^-$)‡ | 3 | 71 | 1.1 |

Reactions conditions: Weight of the catalyst is 0.1 g, 3 mmol of benzaldehyde dimethylacetal, 2 mL of $CH_3NO_2$. 3 mmol of $H_2O$. Reflux for 48 h under $N_2$ atmosphere. ‡50 % of the $Cl^-$ ions were replaced with $OH^-$ ions.

**Table 4**

| Catalyst | Acidity ($mmolg^{-1}$) | | | | | Basicity ($mmolg^{-1}$) | | | | |
|---|---|---|---|---|---|---|---|---|---|---|
| | $H_0 \leq -3.3$ | $H_0 \leq 1.5$ | $H_0 \leq 3.3$ | $H_0 \leq 4.0$ | $H_0 \leq 6.8$ | $H_0 \geq -3.3$ | $H_0 \geq 1.5$ | $H_0 \geq 3.3$ | $H_0 \geq 4.0$ | $H_0 \geq 6.8$ |
| α FeOOH | 6.03 | 10.72 | 10.05 | 6.7 | 0.67 | 0 | 0.07 | 0 | 0 | 0 |
| β FeOOH | 1.67 | 8.71 | 10.59 | 4.02 | 0.34 | 0 | 0.33 | 0 | 0.01 | 0.001 |
| γ FeOOH | 5.36 | 10.05 | 10.32 | 3.35 | 0.34 | 0 | 0.13 | 0 | 0.01 | 0 |
| δ FeOOH | 4.35 | 9.38 | 10.18 | 3.35 | 0.4 | 0 | 0.33 | 0 | 0 | 0 |